HHS Public Access

Author manuscript

Nat Med. Author manuscript; available in PMC 2010 May 01.

Published in final edited form as:

Nat Med. 2009 November ; 15(11): 1289–1297. doi:10.1038/nm.2021.

NOTCH3 SIGNALING IS REQUIRED FOR THE DEVELOPMENT OF PULMONARY ARTERIAL HYPERTENSION

Xiaodong Li, M.D., Ph.D.[1], **Xiaoxue Zhang, M.D.**[1], **Robin Leathers, B.S.**[1], **Ayako Makino, Ph.D.**[2], **Chengqun Huang, M.D., Ph.D.**[1], **Pouria Parsa, M.D.**[1], **Jesus Macias, Ph.D.**[3], **Jason X.-J. Yuan, M.D., Ph.D.**[2], **Stuart W. Jamieson, M.B., F.R.C.S.**[1], and **Patricia A. Thistlethwaite, M.D., Ph.D.**[1]

[1] Division of Cardiothoracic Surgery, University of California, San Diego, San Diego, CA 92103-8892

[2] Division of Pulmonary and Critical Care Medicine, University of California, San Diego, San Diego, CA 92103-8892

[3] Department of Pathology, University of California, San Diego, San Diego, CA 92103-8892

SUMMARY

Notch receptor signaling is implicated in controlling smooth muscle cell proliferation and maintaining smooth muscle cells in an undifferentiated state. Pulmonary arterial hypertension is a disease characterized by excessive vascular smooth muscle cell proliferation in small pulmonary arteries, leading to elevation of pulmonary vascular resistance with consequent right ventricular failure and death. Here we show that human pulmonary hypertension is characterized by overexpression of *NOTCH3* in small pulmonary artery smooth muscle cells, and that severity of disease in humans and rodents correlates with the amount of Notch3 protein in the lung. We further demonstrate that mice with homozygous deletion of *Notch3* do not develop pulmonary hypertension in response to hypoxic stimulation. We report that pulmonary hypertension can be successfully treated in rodents by administration of DAPT, a γ-secretase inhibitor that blocks activation of Notch3 in smooth muscle cells. We demonstrate a mechanistic link between NOTCH3 receptor signaling through HES5 and smooth muscle cell proliferation and a shift to an undifferentiated smooth muscle cell phenotype. These data suggest that the NOTCH3-HES5 signaling pathway is crucial for the development of pulmonary arterial hypertension and provides a target pathway for therapeutic intervention.

Changes in the structure, function, and integrity of blood vessels are necessary to the pathogenesis of many diseases, including pulmonary arterial hypertension (PAH), atherosclerosis, and neointimal repair. Adult vascular smooth muscle cells (vSMCs) are not

Address Correspondence to: Patricia A. Thistlethwaite M.D.-Ph.D., Division of Cardiothoracic Surgery, University of California, San Diego, San Diego, CA 92103-8892, Phone: 619-543-7777, Fax: 619-543-2652, pthistlethwaite@ucsd.edu.

AUTHOR CONTRIBUTIONS

X.L. and P.T. designed the research. X.L., X.Z., R.L., A.M., C.H., P.P., and J.M. performed the experiments. J.Y. and S.J. assisted with data analysis and review of the manuscript. X.L., X.Z., and P.T. prepared the figures. P.T. wrote the manuscript.

terminally differentiated and are capable of modulating their phenotype in response to exogenous stimuli, cell-cell interaction, and cell-matrix signaling1. However, little is known regarding genetic pathways which regulate plasticity and proliferation of pulmonary vSMCs *in vivo*.

An excellent model system for study of vSMC plasticity is the human disease, PAH. This disease is characterized by structural remodeling of small pulmonary arteries and arterioles, causing vessel wall thickening and luminal occlusion by vSMC and endothelial cell proliferation2. PAH vasculopathy is progressive, diffuse, and eventually results in obliteration of the distal pulmonary arterial tree. Clinically, PAH results in elevation of pulmonary arterial pressures (PAP), leading to right ventricular failure and death. It afflicts approximately 100,000 individuals and is the cause of death in 20,000 people each year in the United States3. Although certain conditions, such as hypoxia, fenfluoramine ingestion, collagen vascular disease, portal hypertension, and intracardiac left-to-right shunting are stimuli for this disease4, the mechanism of how the lung remodels its vSMC architecture in small pulmonary arteries in PAH remains unknown.

Recently, Notch3, a member of the Notch family receptors, has been implicated in controlling vSMC proliferation and differentiation. The Notch receptors (Notch1–4) are single transmembrane-spanning proteins that receive signals from cell-bound ligands encoded by the *Jagged* (*Jag1*, *Jag2*) and *Delta-like* (*Dll1*, *Dll3*, and *Dll4*) gene families, and thus function by direct cell-cell contact or autocrine stimulation5. After ligand binding, Notch receptors undergo several proteolytic events that lead to release of the intracellular domains (ICD) of these receptors. The Notch ICD translocates to the nucleus, where it forms an active transcriptional complex with the DNA binding protein, C-promoter-binding factor-1, CBF1 (also known as recombination signal binding protein for immunoglobulin kappa J region, Rbpj), mastermind-like 1 (Maml1) protein, and histone acetyltransferases, to regulate cell fate and differentiation decisions. The key downstream genes of Notch signaling are the *Hes (Hairy/Enhancers of Split)* and *Hrt (Hairy-related)* gene families, which when activated by Notch, reduce expression of downstream transcriptional effectors like Mash6, myoD7, and myocardin8, as well as cell-cycle regulatory proteins, $p27^{kip1}$ 9 and $p21^{waf1/cip1}$ 10. Notch signaling has also been found to directly modulate the expression of the platelet-derived growth factor receptor-β11.

Several lines of evidence suggest that Notch3 signaling regulates arterial SMC identity, proliferative capacity, and anti-apoptotic activity. First, Notch3 signaling is critical in determining lineage fate of arterial SMCs in the late developing embryo12. Second, Notch3 is expressed exclusively on vSMCs in the adult, and expression of this gene has been linked to modulation of non-pulmonary vSMCs into an undifferentiated state13,14. Third, targeted mutagenesis in mice disrupting *Notch3* results in failure of maturation of vSMCs in small arteries/arterioles15. Fourth, *NOTCH3* mutations in humans result in CADASIL (cerebral autosomal dominant arteriopathy with subcortical infarcts and leukoencephalopathy), a disease characterized by vSMC death in small arteries in the brain, leading to obliteration of the cerebral circulation and brain infarction16.

Since PAH is a disease characterized by excessive vSMC proliferation, we tested the hypothesis of direct involvement of NOTCH3 in the development of this disease.

RESULTS

Notch3 is a marker for PAH and PH disease severity

To investigate the expression pattern of Notch3 in normal and pulmonary hypertensive lungs, we examined lung biopsies from 20 individuals with non-familial PAH undergoing lung transplantation compared to biopsies from 20 non-pulmonary hypertensive individuals, 20 mice with hypoxia-induced PH compared to 20 control littermates, and 20 rats with monocrotaline-induced PH compared to 20 control littermates (Fig. 1a,b). We found elevated levels of Notch3 mRNA and ICD protein in human and rodent pulmonary hypertensive lung tissues compared to normotensive lung samples. To characterize whether augmented Notch3 levels were specific to lung in PH, we compared organ-specific levels of Notch3 between normal and pulmonary hypertensive mice (Fig. 1c). *Notch3* mRNA levels were higher in the lung, brain, heart, and kidney in animals exposed to 10% oxygen for 6 weeks (pulmonary hypertensive animals) compared to normoxic animals (non-pulmonary hypertensive animals) (Fig. 1c, left panel). However, levels of Notch3 ICD protein were minimally detected in most organs, while lung levels of Notch3 ICD protein more than tripled in animals with hypoxia-induced PH (Fig. 1c, right panel).

To test whether Notch3 expression correlated with disease progression, we studied humans with varying degrees of PAH, as well as rodents at serial timepoints during hypoxia-induced or monocrotaline-induced PH. In human subjects, NOTCH3 levels in the lung correlated directly with the severity of PAH as measured by pulmonary vascular resistance (PVR) (Fig. 1d). For rodents, gene expression analysis (Fig. 1d,e) and PAP measurements (Supplementary Table 1) were performed at serial timepoints after institution of 10% oxygen or monocrotaline injection. There was increase in expression of Notch3 in the lung as a function of time and disease severity for both hypoxia- and monocrotaline-induced PH animals. Hypoxic PH mice had 3-fold higher levels of Notch3 expression at mRNA and protein (ICD) levels in their lungs compared to normoxic animals, and had PAPs consistent with advanced PH. Rats with monocrotaline-induced PH had progressive elevation in steady-state levels of Notch3 mRNA and ICD protein in their lungs compared to controls over the timespan of disease progression. We found no difference in expression of Notch1, 2, or 4 in the lungs of normotensive versus PH animals (data not shown). We also found an increase in Hes5, a downstream effector target of Notch signaling, in human and rodent lungs with PAH/PH (Fig. 1d). High levels of Hes5 in lung tissue correlated with worsening disease severity. In contrast to *Hes5*, we found no difference in expression of the other Notch3 target genes, *Hes1*, *Hes7*, *Hrt1*, *Hrt2*, and *Hrt3*, in the lungs of normotensive versus pulmonary hypertensive humans and rodents (Supplementary Fig. 1). Our results indicate that Notch3 and Hes5 are sensitive markers for the severity of PAH in humans and PH in two rodent models of disease.

Notch3 and Hes5 expression are confined to vSMCs in the lung

Immunofluorescent staining of human and rodent lung demonstrated that Notch3 and Hes5 were confined to vSMCs in small pulmonary arteries measuring <1,500 μm in diameter (Fig. 2a,b). NOTCH3 staining was localized in the media of small pulmonary arteries, with sporadic staining in the neointima (Supplementary Fig. 2). Notch3 and Hes5 staining were not detected in vSMCs from pulmonary veins or venules (data not shown). Greater levels of Notch3 and Hes5 vSMC-specific staining were seen in pulmonary hypertensive lung tissues compared to normotensive, age, and sex-matched control lung tissue in both humans and rodents (Fig. 2a,b).

To characterize differences between PAH and non-PAH vSMCs, we subcultured small pulmonary artery SMCs (sPASMCs) from humans with and without PAH. Analysis of subcultured sPASMCs (isolated from 500–1,500 μm diameter vessels) from individuals with PAH, demonstrated that steady-state levels of NOTCH3 mRNA and protein as well as HES5 mRNA and protein were increased in these cells compared to sPASMCs subcultured from humans without PAH (Fig. 2c,d).

Notch3 increases proliferation in sPASMCs

As vSMC proliferation is one of the underlying mechanisms of vascular remodeling in PAH, we investigated whether constitutive expression of *Notch3 ICD* (via adenoviral gene transduction; see Supplementary Methods) affected proliferation of human sPASMCs. Subcultured sPASMCs infected with Adeno-*Notch3 ICD* exhibited increases in Notch3 ICD protein and Hes5 protein, compared with Adeno-*lacZ*-transduced sPASMCs (Fig. 3a). Analysis of the Notch3 phenotype revealed a significantly increased growth rate at preconfluence (Fig. 3b, left panel). Constitutive high-level *Notch3* expression in sPASMCs resulted in increased proliferation as determined by ^{3}[H] leucine incorporation (Fig. 3b, right panel).

HES5 inactivation reverses Notch3 proliferative effect in sPASMCs

To test whether the effect of Notch3 ICD on human sPASMC proliferation was dependent on NOTCH signaling through HES5, we utilized *HES5* siRNA to reduce *HES5* expression. Transfection of *HES5* siRNA into vSMCs constitutively expressing Notch3 ICD significantly decreased *HES5* expression (Fig. 3c) and ^{3}[H] leucine incorporation (Fig. 3d, right panel); both were unaffected in vSMCs constitutively expressing Notch3 ICD transfected with a scrambled oligonucleotide. Knockdown of *HES5* abolished the proliferative effect of Notch3 ICD in sPASMCs (Fig. 3d). These results suggest that an upregulated NOTCH3-HES5 signaling pathway plays an important role in the proliferation of human sPASMCs, and inhibition of HES5 can attenuate this process.

Proliferation of sPASMCs from PAH lungs is dependent on NOTCH3-HES5

Analysis of sPASMCs from ten human subjects with idiopathic PAH or without PAH, allowed us to compare growth rates and gene expression patterns between cells from these two populations. We found that sPASMCs from PAH subjects had lower levels of several contractile SMC markers (*SMOOTHELIN* and *MHC*) compared to sPASMCs from non-

PAH individuals, while the contractile protein, α-smooth muscle-actin (*α-SM-ACTIN*) and *CALPONIN* were slightly increased in PAH vSMCs compared to non-PAH vSMCs (Fig. 4a). sPASMCs from PAH lungs demonstrated significantly shorter doubling times and higher rates of ^{3}[H] leucine incorporation compared to sPASMCs from non-PAH lungs (Fig. 4b).

To test whether HES5 contributed to the enhanced *in vitro* proliferative rate of sPASMCs from PAH versus non-PAH human subjects, we used *HES5* siRNA to knockdown this gene product (Fig. 4c). Inhibition of *HES5* expression markedly attenuated PAH vSMC proliferation and ^{3}[H] leucine incorporation, suggesting that NOTCH signaling through HES5 may play a role in the development of pulmonary medial hypertrophy (Fig. 4d). siRNA knockdown of *HES5* in PAH sPASMCs also resulted in increased expression of vSMC contractile markers, *MHC* and *SMOOTHELIN*, over that seen in untreated or scrambled-treated PAH sPASMCs (Fig. 4a,e). These observations suggest that enhanced NOTCH signaling through HES5 seen in PAH vSMCs may contribute to the ability of these cells to proliferate and lose expression of markers of contractile vSMCs.

Notch3$^{-/-}$ mice are resistant to the development of PH

To test whether Notch3 signaling is requisite for development of PH, we studied *Notch3* knockout mice (with homozygous deletion of *Notch3*, lacking 2.5 kb of genomic sequence encoding epidermal growth factor-like repeats 8–12 in the extracellular domain17) for development of hypoxia-induced PH. *Notch3*$^{-/-}$ mice had minimal expression of Hes5 in the lung in conditions of hypoxia (10% oxygen) and normoxia. In contrast, wildtypelungs demonstrated elevated levels of Notch3 ICD and Hes5 protein when the animals were subjected to hypoxia (Fig. 5a).

Notch3$^{-/-}$ mice did not develop elevated right ventricular systolic pressures (RVSP) over a 6-week hypoxic period (Fig. 5b). In contrast, wildtype and *Notch3*$^{+/-}$ littermates manifested progressively elevated RVSP, with a mean increase from 18.6 mmHg to 32.5 mmHg (wildtype) and 18.8 mmHg to 34.6 mmHg (heterozygous) over 6 weeks of hypoxia. *Notch3*$^{+/+}$ and *Notch3*$^{+/-}$ animals developed abnormal small pulmonary artery muscularization and luminal narrowing consistent with advanced PH, while *Notch3*$^{-/-}$ mice had normal appearing small arteries without excessive muscular thickening (Fig. 5c). Expression of proliferating cell nuclear antigen (PCNA) was decreased in small pulmonary arteries in *Notch3*$^{-/-}$ mice compared to wildtypes at 4 and 6 weeks in hypoxia (Fig. 5c,d). Changes in wall thickness and morphology were quantified for small pulmonary arteries in the range of 15–250 μm diameter for *Notch3*$^{-/-}$, *Notch3*$^{+/-}$, and *Notch3*$^{+/+}$ mice (Supplementary Table 2a). Pulmonary vessel medial thickening during hypoxia correlated directly with cellular proliferation as measured by the number of cells positively stained for PCNA for wildtype animals (Fig. 5c,d; Supplementary Table 2a). *Notch3*$^{-/-}$ mice had absence of medial thickening of pulmonary arterioles/small arteries and had minimally-detectable PCNA staining in lung vSMCs. Vessel/alveoli ratios were not significantly different between *Notch3*$^{-/-}$ and *Notch3*$^{+/+}$ or *Notch3*$^{+/-}$ mice (Supplementary Table 2a).

Notch3$^{-/-}$ mice, maintained in hypoxia for 6 weeks, had normal pulmonary angiograms with diffuse vascular blush, while wildtype littermates had angiograms demonstrating severe

small-vessel pruning similar to that seen in human PAH (Fig. 5e). Absence of PH in *Notch3*$^{-/-}$ mice was confirmed by cardiac measurements of chamber weight. Right ventricular weight to that of the left ventricle and septum, as an index of right ventricular hypertrophy, was constant in *Notch3*$^{-/-}$ mice, while increased chronically-hypoxic *Notch3*$^{+/+}$ and *Notch3*$^{+/-}$ animals (Fig. 5f).

To examine whether absence of PH in *Notch3*$^{-/-}$ mice was due to inhibition of pulmonary vasoconstriction, alterations in pulmonary vessel myogenic tone, or changes in pulmonary vasoreactivity to pulmonary blood flow, we did four sets of experiments. First, we compared agonist-mediated vasoconstriction in isolated intrapulmonary small arteries between *Notch3*$^{-/-}$ mice and wildtype littermates. As shown in Supplementary Fig. 3a, the active tension induced by high K^+ and prostaglandin $F_{2\alpha}$ in pulmonary arterial rings was not affected in *Notch3*$^{-/-}$ mice compared to rings from *Notch3*$^{+/+}$ mice. Second, to assess the relationship between myogenic tone and pulmonary blood flow in *Notch3*$^{+/+}$ and *Notch3*$^{-/-}$ mice, we studied pressure-flow relationships in an isolated ventilated, perfused lung system18. We found that in both *Notch3*$^{+/+}$ and *Notch3*$^{-/-}$ mouse lungs, incremental increases in pulmonary blood flow caused similar augmentation of PAP (Supplementary Fig. 3b). Third, we measured pulmonary and systemic hemodynamic response to an acute vasodilator, intravenous epoprostenol, in *Notch3*$^{+/+}$ and *Notch3*$^{-/-}$ normoxic and chronically-hypoxic mice (Supplementary Fig. 4). Under normoxic conditions, *Notch3*$^{+/+}$ and *Notch3*$^{-/-}$ mice had no difference in pulmonary vasoreactivity to vasodilator infusion and had similar baseline measurements for PAPs and total PVR (TPVR). Chronically-hypoxic *Notch3*$^{+/+}$ mice had less change in mean PAP and TPVR in response to vasodilator challenge, suggesting that their PH is, in part, “fixed” due to small vessel pathologic changes, rather than to altered vasoreactivity. In contrast, *Notch3*$^{-/-}$ mice, which did not develop PH after 6 weeks of hypoxia, had similar baseline measurements and vasoreactivity to vasodilator challenge compared to normoxic *Notch3*$^{+/+}$ and *Notch3*$^{-/-}$ mice. Fourth, we performed electron microscopy to analyze vSMCs within the media of small pulmonary arteries of *Notch3*$^{+/+}$ and *Notch3*$^{-/-}$ mice (Supplementary Fig. 5). Structural abnormalities in vSMCs from tail and cerebral arteries of *Notch3*$^{-/-}$ mice have been speculated to account for altered flow-induced vasoreactivity in these vessels19. However, we found no difference in vSMC morphology in small pulmonary arteries from *Notch3*$^{+/+}$ and *Notch3*$^{-/-}$ mice, suggesting that Notch3 may play different roles in vasomotor tone in the systemic and pulmonary circulations. Collectively, our results demonstrate that Notch3 signaling is mainly involved in pulmonary vascular remodeling, rather than in affecting pulmonary vasoreactivity.

In vivo inhibition of Notch3 cleavage reverses PH in rodents

The γ-secretase inhibitor DAPT (N-[N-(3,5-diflurophenacetyl)-L-alanyl]-S-phenylglycine *t*-butyl ester) has been shown to block the *in vitro* and *in vivo* cleavage of Notch proteins to ICD peptides20. We tested our hypothesis that Notch3 signaling is required for development of PH, and that chemical blockade of Notch3 cleavage would effectively treat and reverse this disease. Dose-response experiments were performed to determine the effective ED_{50} for blockage of Notch3 cleavage in the lung. We induced hypoxic PH in mice and subsequently treated them with a daily subcutaneous dose of 10 mg kg^{-1} DAPT from day 15–42 while

they were in 10% oxygen. Although gastrointestinal side effects have been reported with γ-secretase inhibitors in rodents21, we did not observe any clinical side effects with DAPT administration at this dose. Verification of inhibition of Notch3 cleavage in lung tissue was done by Western blotting (Fig. 6a) and immunohistochemistry (Fig. 6b) at biweekly intervals during DAPT administration. At timepoints after institution of hypoxia, before and after DAPT treatment, we examined RVSP and systemic arterial blood pressures (SBP) of DAPT-treated and saline-treated controls (Fig. 6c). Administration of DAPT reversed hypoxia-induced PH. Animals receiving this drug, from days 15–42 while in the hypoxia chamber, had significant reductions in RVSP relative to SBP, while control animals, which did not receive DAPT, developed PH with elevated RVSPs. By quantifying muscularization and morphology of the distal pulmonary vessels, we found that mice treated with DAPT had normal appearing pulmonary vessels with rarely detected medial thickening or vessel occlusion (Fig. 6d, Supplementary Table 2b). Sham-treated animals developed progressive medial thickening of small pulmonary arteries/arterioles consistent with the usual pattern of PH development in hypoxic animals. Using staining for PCNA, we showed minimal proliferating vSMCs in the walls of small pulmonary arteries of DAPT-treated animals, compared to sham-treated controls (Fig. 6d). Furthermore, we showed that treatment with DAPT increased the number of apoptotic cells in the remodeled small pulmonary arteries in chronically hypoxic animals (Fig. 6e). These results indicate that the therapeutic effect of DAPT on hypoxia-induced PH involves both anti-proliferative and pro-apoptotic effects on sPASMCs.

Mice angiograms performed in chronically-hypoxic, DAPT-treated animals demonstrated diffuse vascular blush consistent with a patent distal pulmonary vascular tree, while angiograms performed in control animals showed blunting of the pulmonary vasculature with absence of peripheral artery filling (Fig. 6f). Vessel/alveoli ratios were not significantly different between hypoxic DAPT-treated and DMSO-treated mouse lungs, suggesting that vascular pruning seen on angiography in control animals was due to vessel stenosis/occlusion rather than vessel loss (Supplementary Table 2b). Mice treated with DAPT had regression of right ventricular hypertrophy, further indicating that they were effectively treated for PH (Fig. 6g).

DISCUSSION

Biochemical, genetic, and clinical evidence indicates that SMC proliferation in small pulmonary vessels is an essential part of the pathogenesis of pulmonary hypertension. This study identifies Notch3 as a crucial mediator of proliferation of sPASMCs and a crucial mediator for development of rodent PH, and possibly human PAH.

Our goal has been to understand the molecular basis by which normal pulmonary vessels develop smooth muscle hyperplasia and medial thickening which eventually occlude the distal pulmonary arterial tree and cause clinical manifestations of PAH. As a result of the work reported, we have four major conclusions. First, human PAH vasculopathy is characterized by high steady-state levels of NOTCH3 and its downstream effector, HES5, in SMCs lining small pulmonary arteries/arterioles. Our results establish a link between Notch3 signaling and the magnitude of PH in humans and animals. We demonstrate that the

level of Notch3 protein is a sensitive molecular marker of severity of PAH in humans and PH in rodents. Second, constitutive Notch3 ICD expression induces sPASMC proliferation. This notion, coupled with the finding that NOTCH3 is overexpressed at mRNA and protein levels in the lungs of humans with PAH, support a potentially critical role of NOTCH signaling in mediating vSMC proliferation seen in this disease. To our knowledge, these findings are the first description of NOTCH/HES5 signaling in the adult lung vasculature. Our results establish a link between NOTCH3 signaling and the coordinate regulation of HES5 effector expression in the context of vSMC proliferation. We found that siRNA inhibition of *HES5* expression causes a decrease in sPASMC proliferation and a shift in gene expression in vSMCs toward a more differentiated phenotype. Third, we show that Notch3 is requisite for the development of hypoxic PH in rodents. *Notch3*$^{-/-}$ mice are resistant to development of PH and are unable to generate a medial hypertrophic response to hypoxia, because Notch3-mediated proliferative and possibly antiapoptotic effect on sPASMC is required for the development of pulmonary vascular medial hypertrophy. Finally, we demonstrate that rodent PH can be effectively treated by blocking Notch3 signaling. Collectively, these results suggest that Notch3 signaling is required for the clinical and pathologic development of PAH/PH.

In the early stages of human PAH, the disease has two components: pulmonary vasoconstriction and vascular remodeling. As the disease progresses, the capacity of the pulmonary vascular bed to dilate and recruit unused vasculature is lost22–25. Recently, Chantemele et al.19 suggested that Notch3 deficiency causes reduction in pressure-induced myogenic tone and enhanced flow-mediated dilation in tail artery of the rat, which is associated with reduction in RhoA activity. Broughton et al.26 has found that chronic-hypoxic rats have increased myogenic tone in small pulmonary arteries through a ROK-dependent myofilament Ca^{2+} sensitization. These results raise the possibility that Notch3 may modulate not just pulmonary vessel wall remodeling, but may also influence pulmonary vascular tone and dilation. Our results examining Notch3 in the pulmonary circulation have revealed little difference between *Notch3*$^{+/+}$ and *Notch3*$^{-/-}$ mice with regards to response to vasoconstrictor drugs, flow-induced changes in pressure, and response to pulmonary vasodilators. Collectively, these results suggest that Notch3 may play different roles in the pulmonary and systemic circulations.

Clues as to why NOTCH3 may play a role in PAH come from studies of Notch function in modulating vSMC phenotype, its involvement with bone morphogenetic protein (BMP) signaling, and its role in the vessel wall in the setting of hypoxia. Notch-Hes/Hrt signaling has been associated with lack of cell cycle arrest in aortic SMCs9,13, has been reported to repress myocardin-induced differentiation of myofibroblasts8, and has been found to regulate SMC proliferation in neointimal injury in Hrt2-deficient and Notch1$^{+/-}$ mice27,28. Although these studies suggest a role of Notch signaling in SMC proliferation-homeostasis, none have been done in sPASMCs. One of the paradigms of Notch signaling is the observation that the biologic response to receptor activation is dependent on dosage as well as cellular and organ context29. It is difficult to extend findings from different vascular beds or immortalized cell lines to the behavior of SMCs from the distal pulmonary vascular tree.

Notch3 may affect sPASMC remodeling in PH due to crosstalk with the Bmp receptor (Bmpr) signaling pathway. *BMPR2* mutations have been found to be associated with the development of a familial human PAH30. However, 40% of familial PAH individuals do not harbor mutations in *BMPR2*, and most non-familial cases lack association with *BMPR2* mutation31. This suggests that alternate or convergent pathways to BMPR signaling may play a role in this disease. Recently, signal integration between Notch and Bmpr has been found in several organs and cell types. Activation of Bmp signaling has been found to lead to enhanced transcription of the Notch target gene *Herp2* (*Hrt1*), through binding of the intracellular Bmp-mediated transcription factor, Smad1, with Notch ICD32–34. Interestingly, Hrt1 was then found to efficiently bind to and induce degradation of Id1, a downstream effector of Bmp signaling. Protein-protein interactions between Id2 (in Bmpr/Id signaling) and Hes1 (in Notch signaling) have also been demonstrated in the chicken hindbrain to be key regulators of expression of genes involved in neurogenesis33. These feedback loops provide evidence that Notch signaling, in the context of certain organs, may modulate downstream Bmpr signaling.

A second line of evidence suggesting that NOTCH signaling may be essential to the development of PAH is its role in hypoxia, a known environmental inducer of this disease. Hypoxia is known to promote the undifferentiated cell state in various stem cell and precursor populations35. A recent report shows that hypoxia requires functional Notch signaling to maintain cells in an undifferentiated state36. In a mechanism similar to the crosstalk between Bmpr and Notch signaling, hypoxia inducible factor1-α (Hif1-α), an intracellular mediator of oxygen sensing, has been found bind to Notch ICD and act as a co-enhancer to stimulate transcription of Notch responsive genes under hypoxic conditions. Thus, NOTCH ICD is at the convergence point of two different signaling mechanisms: hypoxic HIF1-α signaling and BMP signaling, both of which have implicated in the development of PAH.

In summary, we find that high steady-state levels of NOTCH3 are associated with the development of PAH in humans and that Notch3 expression is obligate for the development of PH in two experimental models of this disease. Our work demonstrates that constitutive NOTCH3 signaling induces pulmonary vSMCs into a proliferative phenotype and that pulmonary hypertensive vascular pathology *in vivo* can be prevented by treatment with a drug that blocks Notch signaling. It is possible that other Notch receptors may also play a role in the development of PH, and more specific inhibitors of Notch3 signaling will need to be tested in the treatment of this disease. Our results suggest that molecular targeting of the NOTCH3-HES5 axis in pulmonary vascular smooth muscle may be a novel strategy for treatment of PAH based on the genetic profile of the pulmonary vascular wall in this disease. Future inhibition of the expression or effect of NOTCH3 signaling in the adult pulmonary vasculature may be a useful strategy to prevent and treat PAH in humans.

METHODS

Human tissue processing

Human pulmonary and systemic arterial pressures were measured by a Swan-Ganz catheter and radial arterial line. After sternotomy or thoracotomy, a 4 cm biopsy was taken from a

lobe of both the right and left lungs before cardiopulmonary bypass and during ventilation with 100% oxygen. Tissue was collected from 20 human subjects with non-familial PAH undergoing lung transplantation23. PAH individuals had systolic PAP > 80 mmHg and PVR ≥620 dynes sec^{-1} cm^{-5}. Tissue was collected from 20 individuals without PAH (mean PAP < 20 mmHg, PVR < 220 dynes sec^{-1} cm^{-5}) undergoing lung resection for benign nodules. All subjects had given consent for lung biopsy. The study was approved by the UCSD Institutional Review Board, and experiments were performed within relevant guidelines and regulations of this body.

Hypoxia

Animal experiments were approved by the UCSD Animal Subject's Committee, and were performed in accordance with the relevant guidelines and regulations of this body. Normobaric hypoxic chambers maintained with 5.5 L min^{-1} flow of hypoxic air (10% O_2 and 90% N_2) were opened twice a week for cleaning and replenishment of food and water. Oxygen concentrations were monitored continuously with blood gas analyzers, and soda lime was used to reduce the concentration of carbon dioxide. For normoxic conditions, mice were kept in the same room with the same 12-hour-light-12-hour-dark cycle.

For wildtype mouse experiments (Fig. 1)—8-week old female *C57/Bl6* mice were kept in either 10% oxygen or in room air (21% oxygen). At 0, 4, and 6 weeks (20 animals in each group for each timepoint), animals were sacrificed for analysis.

For knockout mouse experiments (Fig. 5)—8-week old female *C57/Bl6 Notch3*$^{-/-}$ mice as well as *Notch3*$^{+/+}$ and *Notch3*$^{+/-}$ female littermates were maintained in 10% oxygen for 0, 4, or 6 weeks. 20 wildtype, 20 knockout animals, and 20 heterozygous knockout animals were examined for each timepoint.

For DAPT experiments (Fig. 6)—8-week old female *C57/Bl6* mice were divided into eight groups, each containing 20 animals. Baseline histology, angiography, cardiac weights, and systemic/pulmonary pressures were taken in two groups under normoxic conditions. Six groups were placed in the hypoxia chamber. After 2 weeks in hypoxia, two groups of animals were sacrificed for analysis. The remaining four groups in the hypoxia chamber were randomized to receive a daily subcutaneous injection of 10 mg kg^{-1} of DAPT (Sigma-Aldrich) or DMSO (placebo carrier). At 4 and 6 weeks each, one group of DAPT-treated and one group of DMSO-treated animals were sacrificed for analysis.

Monocrotaline

Adult male *Sprague-Dawley* rats (200–250 g in body weight; Charles River Laboratories) were assigned to either subcutaneous injection of 60 mg kg^{-1} of monocrotaline or saline alone. Hemodyamic measurements and gene expression analysis were performed at 0, 2, and 4 weeks after injection (20 animals per group for each timepoint).

Hemodynamic measurements, pulmonary angiography, and cardiovascular evaluation

We performed rodent hemodynamic measurements and pulmonary angiography as previously described37. For the assessment of right ventricular hypertrophy, the right

ventricle was dissected from the left ventricle and interventricular septum, and these were weighed separately. The weight ratio was then calculated as the ratio of weight of the right ventricle to that of the left ventricle plus the interventricular septum.

Isolation and culture of human sPASMCs

Human sPASMCs were isolated and subcultured from 500–1,500 μm diameter arterioles from PAH and non-PAH subjects as previously described37. Cells were cultured in 5% CO_2 in air at 37 °C in smooth muscle growth medium (SMGM, Cambrex Bioscience) containing 5% fetal bovine serum (FBS). Cells were used in the 4–6th passage. The purity of vSMCs was confirmed by immunohistochemical staining with α-SM-ACTIN, DESMIN, myosin light chain (MLC), and MHC, as well as absence of staining with CD31, CD34, and FACTOR VIII. Greater than 98% of the subcultured vSMCs had positive staining for all four SMC markers.

Smooth muscle cell growth assays

For adenoviral transduction experiments (Fig. 3)—Independent sPASMC subcultures were derived from the lungs of ten individuals without PAH. Human sPASMCs were seeded at 5×10^5 cells per 35 mm diameter well and 12 h later, growth-arrested by washing the cells three times with PBS prior to the addition of SMGM without fetal bovine serum. Cells were incubated at 37 °C, 5% CO_2 for 6 h and then treated with adenoviruses (pAd/CMV/V5-DEST vector [Invitrogen] containing the cytomegalovirus early promoter driving either the mouse *Notch3 ICD* [amino acid sequence in Supplementary Methods] or *Escherichia coli lacZ* gene). For both vectors, 12 independent viral infections per subject's subculture were performed, with multiplicity of infection = 100. For baseline cell counts, 18 h after viral infection, ten wells of transduced cells for each vector type were washed twice with PBS and trypsinized in 150 μl of trypsin/EDTA for 7 min, followed by the addition of 150 μl trypsin neutralizer (Lonza Inc.). The cells were then resuspended and counted in a hemacytometer (ten wells per viral transduction, four counts per well). For the remaining aliquots of cells, after 12–36 h of incubation in SMGM with 5% serum, 1 μCi ml^{-1} of ^{3}[H] leucine was added to each well, and incubation was continued for 8 h. During processing for ^{3}[H] leucine incorporation, the cells from ten wells were counted using a hemacytometer as described above. Twelve independent ^{3}[H] leucine/cell count experiments were performed for each group, with each assay done in triplicate. Values for each group were averaged and presented as mean ± SEM.

For PAH and non-PAH cell experiments (Fig. 4)—sPASMC cell growth assays were performed as above, without the addition of adenoviral vectors.

Histologic and immunohistochemical analyses

After hemodynamic measurements, rodent lungs were prepared by flushing the main pulmonary artery with saline at 20 cm H_2O pressure until the pulmonary venous effluent was cleared of blood. Lungs were fixed in 4% paraformaldehyde, embedded in paraffin, and sectioned at 5 μm thickness. Sections from each animal were stained with hematoxylin and eosin and examined by digital photomicroscopy at various magnifications to determine the severity of PH. A pathologist blinded to the study reviewed ten sections per lung and

determined, for vessels 15–250 μm in diameter, the percentage with medial hyperplasia, the percentage with > 50% luminal stenosis, and the number of myocytes per vessel wall. Vessel/alveoli ratios were determined for small pulmonary arteries 50–1,500 μm in diameter. Immunohistochemical/immunofluorescence experiments were done as previously described38. Antibodies used are described in the supplementary text.

RNA & protein methods

Quantitative reverse transcriptase PCR (qRT-PCR), Northern, and Western blotting were performed as previously described37, 39. For probes, primers, and antibodies used, see supplementary text.

siRNA methods

HES5 siRNA and scrambled control sequences were prepared by Ambion. Three19-nucleotide sequences were selected from the ORF sequence of human *HES5* (GenBank accession no. NM_001010926). A scrambled control oligonucleotide was also generated that bore no significant homology to any mammalian gene sequence. The scrambled oligonucleotide served as a nonsilencing control. Suppression of *HES5* expression by the siRNA oligonucleotides was evaluated in pulmonary vSMCs using Lipofectamine TM RNAiMAX (Invitrogen) as the transfection reagent following suggested protocols. 6 h after transfection, the vSMCs were cultured in SMGM with 5% serum, and later used for smooth muscle cell growth assays, qRT-PCR, or protein assays. Three (siRNA-1, -2, and -3) of the siRNA sequences were evaluated for the efficiency of suppression of HES5 protein and mRNA levels, with siRNA-3 being the most effective (sense: GAGAAAAACCGACUGCGGAtt and antisense: UCCGCAGUCGGUUUUUCUCtt).

Statistical analysis

Data are expressed as mean ± SEM. Statistical significance was determined using one-way ANOVA for multiple group analysis. When two groups with continuous data were compared, statistical differences were assessed with the Wilcoxon rank sum test. The number of animals/samples in each group is indicated in the figure legends or methods.

Supplementary Material

Refer to Web version on PubMed Central for supplementary material.

Acknowledgments

We would like to thank T. Gridley (The Jackson Laboratory) for providing the Notch3 knockout mice strain used in this study. This work was supported by a grant from the US National Institutes of Health (2R01HL70852 to P.T.)

Funding: NIH R01 HL070852 to P.A.T.

References

1. Owens GK, Kumar MS, Wamhoff BR. Molecular regulation of vascular smooth muscle cell differentiation in development and disease. Physiol Rev. 2004; 84:767–801. [PubMed: 15269336]
2. Yuan JX-J, Rubin LJ. Pathogenesis of pulmonary arterial hypertension: the need for multiple hits. Circulation. 2005; 111:534–538. [PubMed: 15699271]

3. Hyduk A, et al. Pulmonary hypertension surveillance – United States, 1980–2002. 2005; 54(SS05): 1–28. http://www.cdc.gov/mmwr/preview/mmwrhtml/ss5405a1.htm.
4. Simonneau G, et al. Clinical classification of pulmonary hypertension. J Am Coll Cardiol. 2004; 43:5S–12S. [PubMed: 15194173]
5. Alva JA, Iruela-Arispe ML. Notch signaling in vascular morphogenesis. Curr Opin Hematol. 2004; 11:278–283. [PubMed: 15314528]
6. de la Pompa JL, et al. Conservation of the Notch signalling pathway in mammalian neurogenesis. Development. 1997; 124:1139–1148. [PubMed: 9102301]
7. Kopan R, Nye JS, Weintraub H. The intracellular domain of mouse Notch: a constitutively activated repressor of myogenesis directed at the basic helix-loop-helix region of MyoD. Development. 1994; 120:2385–2396. [PubMed: 7956819]
8. Proweller A, Pear WS, Parmacek MS. Notch signaling represses myocardin-induced smooth muscle cell differentiation. J Biol Chem. 2005; 280:8994–9004. [PubMed: 15634680]
9. Havrda MC, Johnson MJ, O'Neill CF, Liaw L. A novel mechanism of transcriptional repression of $p27^{kip1}$ through Notch/HRT2 signaling in vascular smooth muscle cells. Thromb Haemost. 2006; 96:361–370. [PubMed: 16953280]
10. Wang W, Prince CZ, Hu X, Pollman MJ. HRT1 modulates vascular smooth muscle cell proliferation and apoptosis. Biochem Biophys Res Comm. 2003; 308:596–601. [PubMed: 12914792]
11. Jin S, et al. Notch regulates platelet-derived growth factor receptor-beta expression in vascular smooth muscle cells. Circ Res. 2008; 102:1483–1491. [PubMed: 18483410]
12. Roca C, Adams RH. Regulation of vascular morphogenesis by Notch signaling. Genes Dev. 2007; 21:2511–2524. [PubMed: 17938237]
13. Campos AH, Wang W, Pollman MJ, Gibbons GH. Determinants of Notch-3 receptor expression and signaling in vascular smooth muscle cells – implications in cell-cycle regulation. Circ Res. 2002; 91:999–1006. [PubMed: 12456485]
14. Morrow D, et al. Notch-mediated CBF-1/RBP-Jk-dependent regulation of human vascular smooth muscle cell phenotype in vitro. Am J Physiol Cell Physiol. 2005; 289:C1188–C1196. [PubMed: 15987768]
15. Domenga V, et al. Notch3 is required for arterial identity and maturation of vascular smooth muscle cells. Genes and Develop. 2004; 18:2730–2735. [PubMed: 15545631]
16. Joutel A, et al. The ectodomain of the Notch3 receptor accumulates within the cerebrovasculature of CADASIL patients. J Clin Invest. 2000; 105:597–605. [PubMed: 10712431]
17. Krebs LT, et al. Characterization of Notch3-deficient mice: normal embryonic development and absence of genetic interactions with a Notch1 mutation. Genesis. 2003; 37:139–143. [PubMed: 14595837]
18. Tuchscherer HA, Vanderpool RR, Chesler NC. Pulmonary vascular remodeling in isolated mouse lungs: effects on pulsatile pressure-flow relationships. J Biomech. 2007; 40:993–1001. [PubMed: 16756983]
19. Chantemele EJ, et al. Notch3 is a major regulator of vascular tone in cerebral and tail resistance arteries. Arterioscler Thromb Vasc Biol. 2008; 28:2216–2224. [PubMed: 18818417]
20. Hellstrom M, et al. Dll4 signaling through Notch1 regulates formation of tip cells during angiogenesis. Nature. 2007; 445:776–780. [PubMed: 17259973]
21. Real PJ, et al. γ-secretase inhibitors reverse glucocorticoid resistance in T cell acute lymphoblastic leukemia. Nat Med. 2009; 15:50–58. [PubMed: 19098907]
22. Eddahibi S, et al. Serotonin transporter overexpression is responsible for pulmonary artery smooth muscle hyperplasia in primary pulmonary hypertension. J Clin Invest. 2001; 108:1141–1150. [PubMed: 11602621]
23. Du L, et al. Signaling molecules in nonfamilial pulmonary hypertension. N Engl J Med. 2003; 348:500–509. [PubMed: 12571257]
24. Hausmann G, et al. An antiproliferative BMP-2/PPARgamma/apoE axis in human and murine SMCs and its role in pulmonary hypertension. J Clin Invest. 2008; 118:1846–1857. [PubMed: 18382765]

25. Thomas M, et al. Activin-like kinase 5 (ALK5) mediates abnormal proliferation of vascular smooth muscle cells from patients with familial pulmonary arterial hypertension and is involved in the progression of experimental pulmonary arterial hypertension induced by monocrotaline. Am J Path. 2009; 174:380–389. [PubMed: 19116361]
26. Broughton BR, Walker BR, Resta TC. Chronic hypoxia induces Rho kinase-dependent myogenic tone in small pulmonary arteries. Am J Physiol Lung Cell Mol Physiol. 2008; 294:L797–L806. [PubMed: 18263668]
27. Sakata Y, et al. Transcription factor CHF/Hey2 regulates neointimal formation in vivo and vascular smooth muscle proliferation and migration in vitro. Arterioscler Thromb Vasc Biol. 2004; 24:2069–2074. [PubMed: 15345511]
28. Li Y, et al. Smooth muscle Notch1 mediates neointimal formation after vascular injury. Circulation. 2009; 119:2686–2692. [PubMed: 19433762]
29. Morrow D, et al. Notch and vascular smooth muscle phenotype. Circ Res. 2009; 103:1370– 1382. [PubMed: 19059839]
30. Deng Z, et al. Familial primary pulmonary hypertension (gene PPH1) is caused by mutations in the bone morphogenetic protein receptor-II gene. Am J Hum Genet. 2000; 67:737–744. [PubMed: 10903931]
31. Lane KB, et al. Heterozygous germline mutations in BMPR2, encoding TGF-beta receptor, cause familial primary pulmonary hypertension. The International PPH Consortium. Nat Genet. 2000; 26:81–84. [PubMed: 10973254]
32. Blokzijl A, et al. Cross-talk between the Notch and TGF-β signaling pathways mediated by interaction of the Notch intracellular domain with Smad3. J Cell Biol. 2003; 163:723–728. [PubMed: 14638857]
33. Bai G, et al. Id sustains Hes1 expression to inhibit precocious neurogenesis by releasing negative autoregulation of Hes1. Develop Cell. 2007; 13:283–297.
34. Kluppel M, Wrana JL. Turning it up a notch: cross-talk between TGFβ and notch signaling. Bioessays. 2005; 27:115–118. [PubMed: 15666349]
35. Lin Q, Lee YJ, Yun Z. Differentiation arrest by hypoxia. J Biol Chem. 2006; 281:30678–30683. [PubMed: 16926163]
36. Gustafsson MV, et al. Hypoxia requires notch signaling to maintain the undifferentiated cell state. Develop Cell. 2005; 9:617–628.
37. Sullivan CC, et al. Induction of pulmonary hypertension by an angiopoietin 1/TIE2/serotonin pathway. Proc Natl Acad Sci. 2003; 100:12331–12336. [PubMed: 14512515]
38. Yu Y, et al. Enhanced expression of transient receptor potential channels in idiopathic pulmonary arterial hypertension. Proc Natl Acad Sci. 2004; 101:13861–13866. [PubMed: 15358862]
39. Zhang L, et al. Gene expression signatures of cAMP/protein kinase A (PKA)-promoted, mitochondrial-dependent apoptosis. Comparative analysis of wild-type and cAMP-deathless S49 lymphoma cells. J Biol Chem. 2008; 283:4304–4313. [PubMed: 18048352]

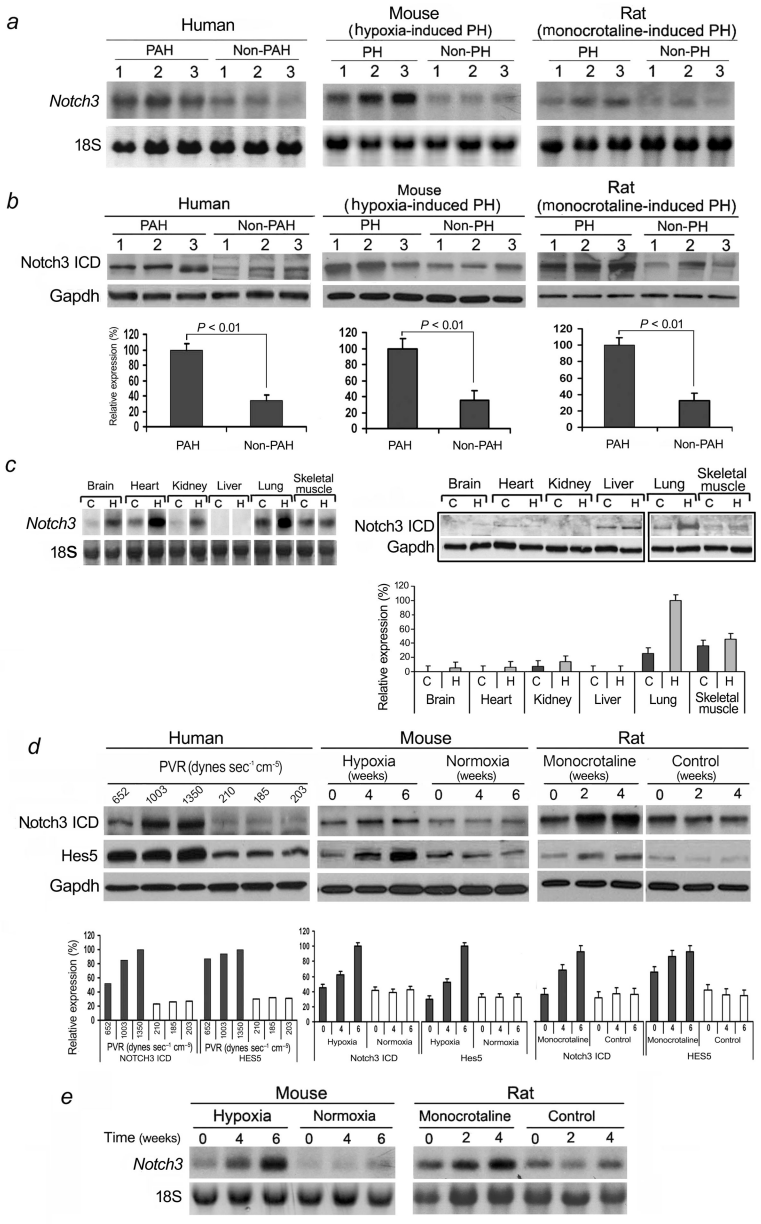

Figure 1.

Notch3 is a marker for PAH and PH disease severity. (**a**) Northern blot analysis of *Notch3* relative to 18S RNA from human lungs with idiopathic PAH (three subjects - left panel), mice with hypoxia-induced PH (three animals - middle panel), and rats with monocrotaline-induced PH (three animals - right panel) compared to control lungs. (**b**) Upper panel: Western blot analysis of Notch3 ICD relative to Gapdh in the same lung tissue as in A. Lower panel: Relative expression values obtained by densitometry of Notch3 ICD protein normalized to Gapdh (n = 20 for each group). (**c**) Northern blot analysis of Notch3 from organs of mice exposed to hypoxia (H) or normoxia (C) for 6 weeks (left panel), Western blot analysis of Notch3 ICD in the same organs (right panel, top). Relative expression values obtained by densitometry of Notch3 protein normalized to Gapdh (n = 4 per group) (right

panel, bottom). (**d**) Western blot analysis of NOTCH3 ICD and HES5 relative to GAPDH in the lungs of subjects with varying severity of PAH and control individuals. PVR = pulmonary vascular resistance (left panel, top). Western blot analysis of Notch3 ICD and Hes5 relative to Gapdh from mouse lungs during development of hypoxia-induced PH, or rat lungs during development of monocrotaline-induced PH, compared to control animals (middle and right panel, top). Lower panel: Relative expression values obtained by densitometry of Notch3 ICD or Hes5 protein normalized to Gapdh (n = 1 for each PVR listed; n = 20 animals for each timepoint). (**e**) Northern blot analysis of total RNA from the lungs of mice and rats as in D.

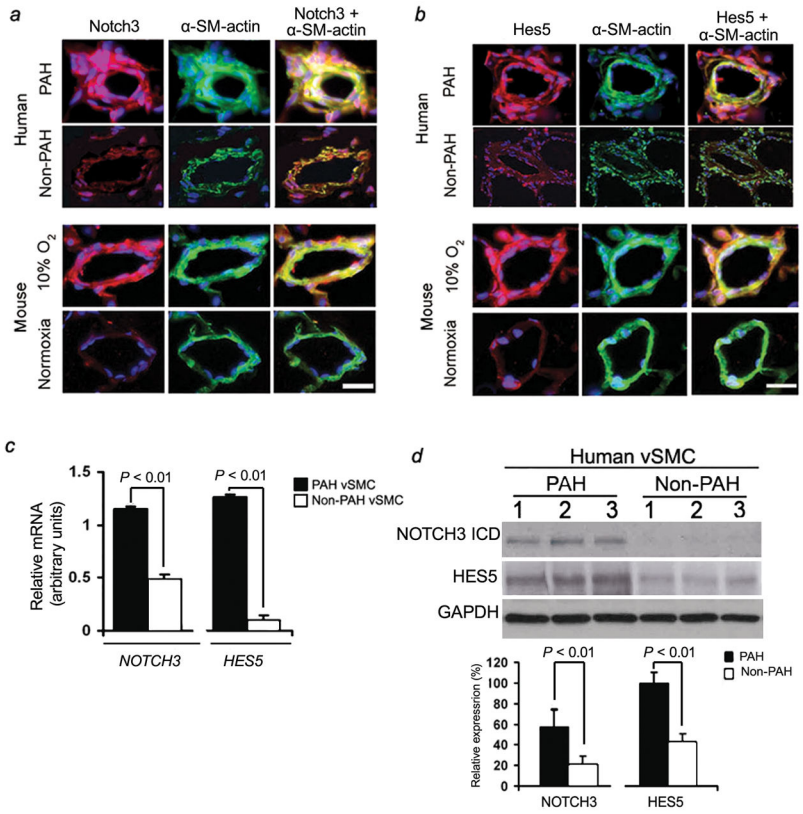

Figure 2.

Notch3 and Hes5 expression are specific to sPASMCs in the lung. (**a**) Notch 3 (red) and α-SM-actin (green) immunofluorescence staining in small pulmonary arteries from humans (top panels) and mice (bottom panels) with and without PAH/PH. Nuclei are counterstained with DAPI (blue). Notch3 staining is confined to sPASMCs and predominates in vessels from PAH/PH lung tissue. Scale bar = 50 μm. (**b**) Hes5 (red) and α-SM-actin (green) immunofluorescence staining in small pulmonary arteries 75–100 μm in diameter in pulmonary hypertensive and normotensive human (top panels) and mouse (bottom panels) lung tissue. Nuclei are counterstained with DAPI (blue). Hes5 staining is confined to sPASMCs and predominates in vessels from PAH/PH lung tissue. Scale bar = 50 μm. (**c**) qRT-PCR analysis of total RNA from subcultured sPASMCs derived from the lungs of ten individuals with and ten individuals without PAH (three subcultures per subject). *NOTCH3* and *HES5* values are normalized to 18S rRNA control. (**d**) Upper panel: Western blot analysis of NOTCH3 and HES5 in subcultured sPASMCs derived from the lungs of three human subjects with and three human subjects without PAH. Lower panel: Relative expression values obtained by densitometric analysis of NOTCH3 and HES5 normalized to GAPDH (*n* = ten PAH subjects' subcultures, *n* = ten non-PAH subjects' subcultures).

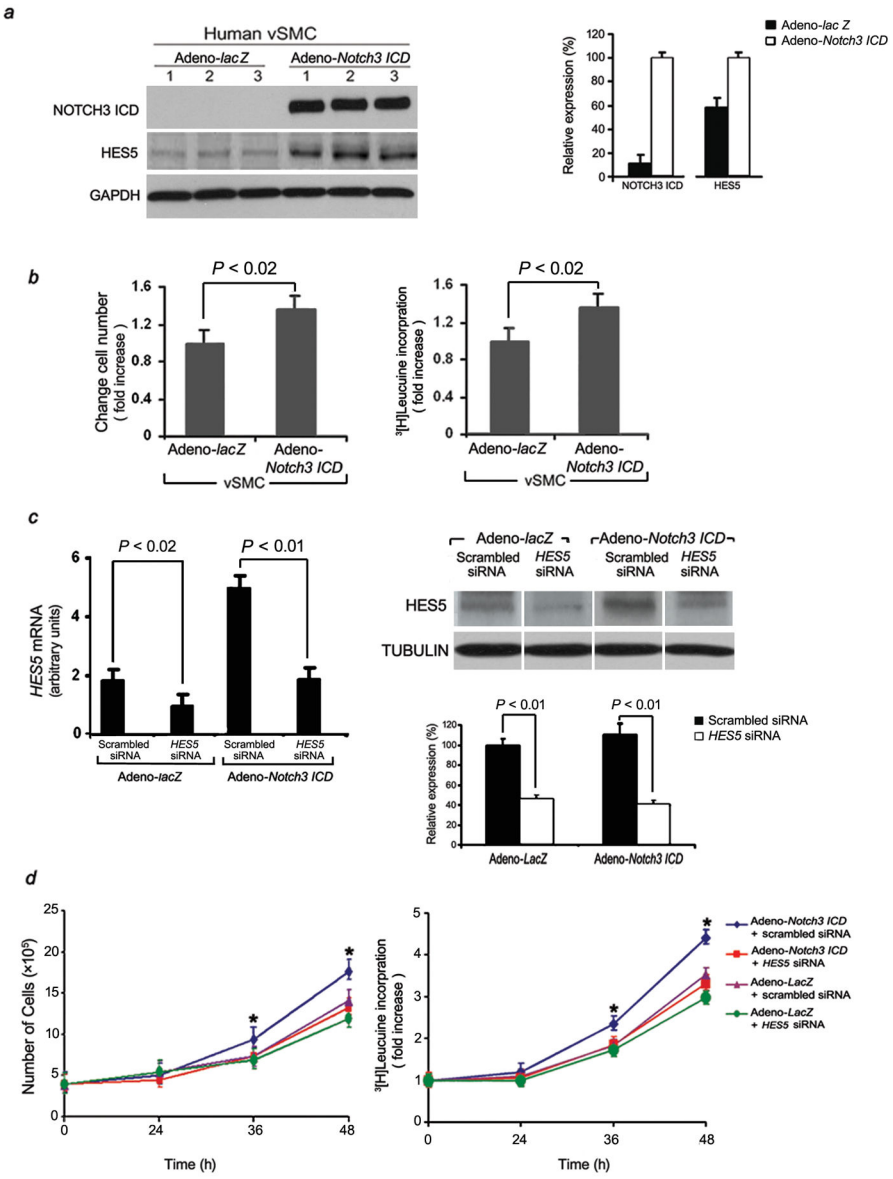

Figure 3.

Notch3 increases vSMC proliferative capacity *in vitro*. (**a**) Left panel: Western blot demonstrating increase in NOTCH3 ICD and HES5 in three sPASMC subcultures (from different individuals) infected with Adeno-*Notch3 ICD* compared to the same subcultures infected with Adeno-*lacZ*. Right panel: Relative expression values obtained by densitometry of Notch3 ICD and HES5 protein normalized to GAPDH (*n* = three subjects' subcultures per group). (**b**) Stimulation of human sPASMC proliferation by constitutive *Notch3 ICD* expression. Left panel: Averaged change in cell number after Adeno-*Notch3 ICD* or Adeno-*lacZ* transduction. (ten human sPASMC subcultures, 12 viral infections per subculture). Right panel: ^{3}[H] leucine incorporation in the same cells as in left panel. (**c**) Effects of *HES5* siRNA and its scrambled control (30 nM). Left panel: qRT-PCR analysis of total RNA from Adeno-*Notch3 ICD*-infected human sPASMCs (*n* = three independent subcultures from ten individuals tested) and control vector-infected SMCs (Adeno-*lacZ; n* = three aliquots of

same subcultures tested) treated with scrambled or *HES5* siRNA. Values are normalized to 18S rRNA control. Right panel, top: Western blot analysis of protein from sPASMCs treated with *HES5* or scrambled RNA after either Adeno-*lacZ* or Adeno-*Notch3 ICD* transfection. Right panel, bottom: Relative expression values obtained by densitometry of HES5 protein normalized to TUBULIN (*n* = three independent experiments for each human subculture, with ten human subcultures per group). (**d**) Left panel: Growth curve of sPASMCs from ten human lungs without PAH (three subcultures per subject), treated with either scrambled or *HES5* siRNA, followed by transfection with either Adeno-*Notch3 ICD* or Adeno-*lacZ*. **P* < 0.01 compared to control groups. Right panel: ^{3}[H] leucine incorporation for the same cells as in left panel. **P* < 0.01 compared to control groups.

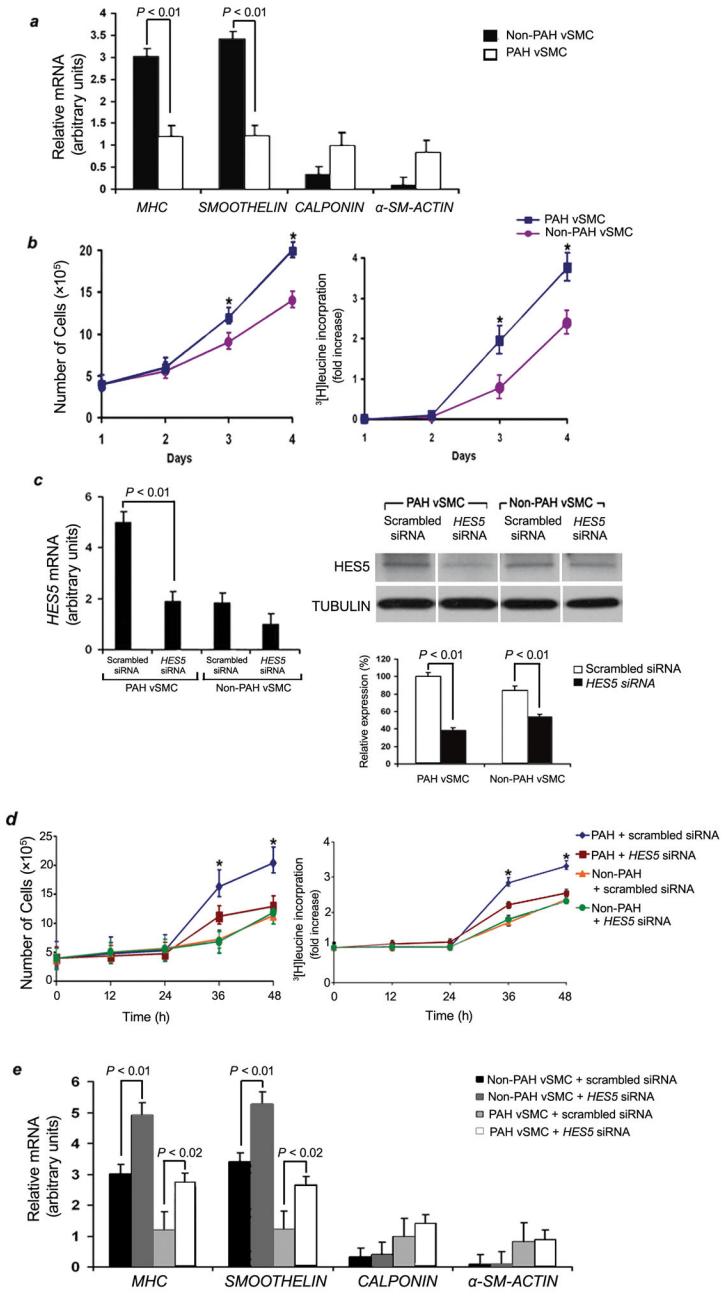

Figure 4.

Faster growth rates and lower levels of contractile vSMC markers in sPASMCs from PAH humans compared with non-PAH subjects are dependent on HES5. (**a**) qRT-PCR analysis of genes associated with vSMC differentiation in sPASMCs (*n* = ten subjects per group, three subcultures per individual) from people with and without PAH. Average expression values are normalized to 18S rRNA. (**b**) Left panel: Growth curves of sPASMCs isolated from human lungs (*n* = ten individuals per group, three subcultures per individual) with and without PAH. **P* < 0.01 versus controls. Right panel: ^{3}[H] leucine incorporation for the same cells as in the left panel. **P* < 0.01 versus controls. (**c**) Effects of *HES5* and scrambled

siRNA (30 nM). Left panel: qRT-PCR analysis of total RNA from PAH and non-PAH sPASMCs (*n* = three independent subcultures from ten humans per group) treated with *HES5* or scrambled siRNA. Values are normalized to 18S rRNA. Right panel, top: Western blot analysis of protein derived from the same cells in the left panel. Right panel, bottom: Relative expression values obtained by densitometry of HES5 protein normalized to TUBULIN (*n* = three independent experiments for each human subculture with ten human subcultures per group). (**d**) Left panel: Growth curve of sPASMCs isolated from the PAH and non-PAH lungs (three subcultures per human subject) treated with either *HES5* or scrambled siRNA. **P* < 0.01 compared to control groups. Right panel: ^{3}[H] leucine incorporation for the same cells as in left panel. **P* < 0.01 compared to control groups. (**e**) Effect of selective knockdown of *HES5* on qRT-PCR measurement of *MHC*, *SMOOTHELIN*, *α-SM-ACTIN*, and *CALPONIN* mRNA in sPASMCs from humans with and without PAH (*n* = ten human subjects per group, three subcultures/human). Data were normalized to 18S rRNA levels and represent means from three independent experiments.

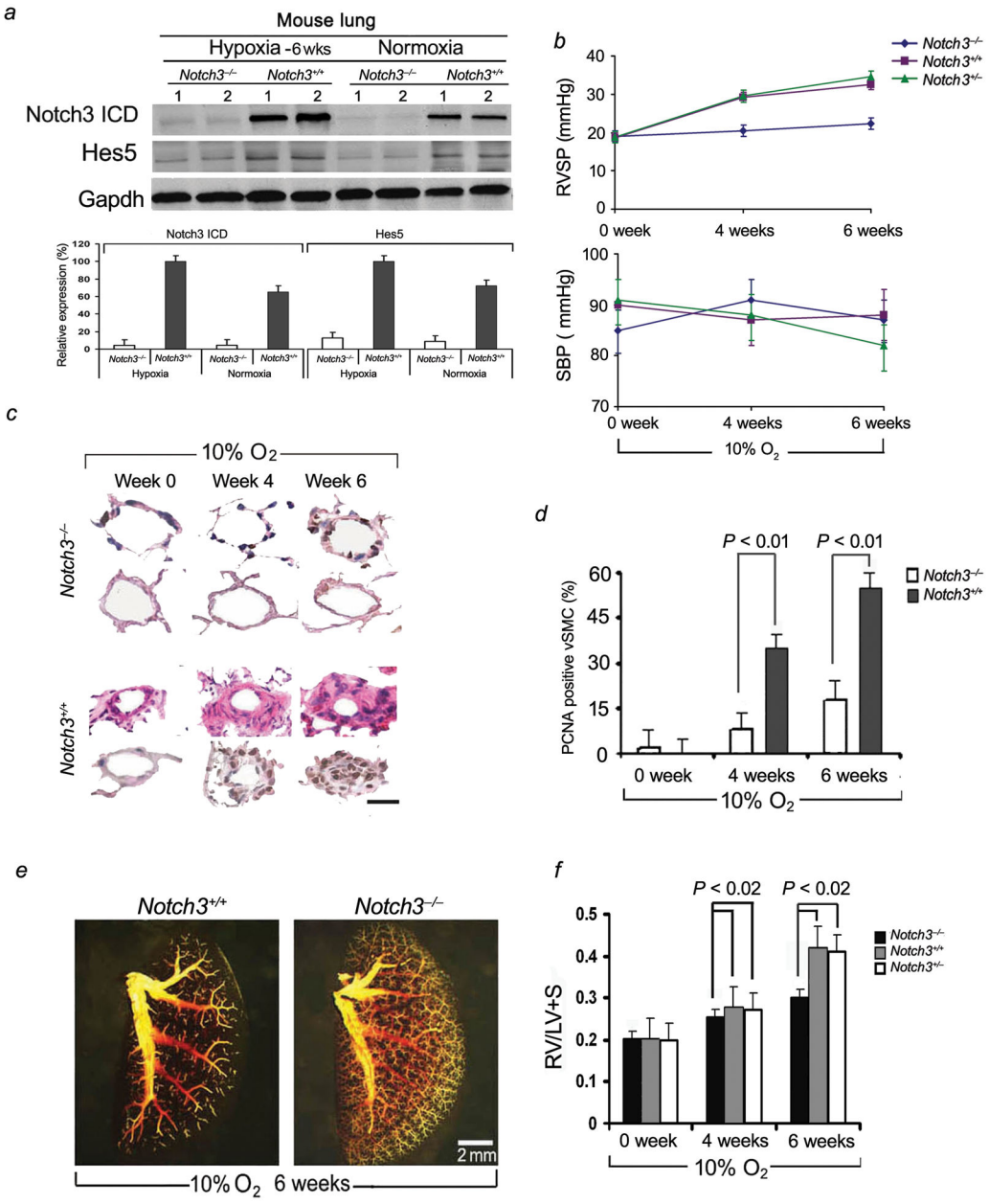

Figure 5.

Notch3$^{-/-}$ mice are resistant to the development of hypoxic PH. (**a**) Upper panel: Western blot analysis of Notch3 ICD and Hes5 in *Notch3*$^{-/-}$ and *Notch3*$^{+/+}$ lung tissues. Lower panel: Relative expression values obtained by densitometry of Notch3 ICD or Hes5 protein normalized to Gapdh (n = 20 per group). (**b**) Averaged SBP and RVSP in *Notch3*$^{-/-}$ mice as well as *Notch3*$^{+/+}$ and *Notch3*$^{+/-}$ littermates at serial timepoints under hypoxic conditions of 10% oxygen (ten readings per animal over one hour, 20 animals per group at each timepoint). (**c**) Hematoxylin and eosin-stained sections (rows one and three) and immunohistochemical analysis of PCNA (rows two and four) of small pulmonary arteries from lungs of *Notch3*$^{-/-}$ and *Notch3*$^{+/+}$ mice after 4 and 6 weeks of hypoxia. Dark nuclei are

PCNA positive. Results are representative sections from at least ten animals per group for each timepoint. Scale bar = 25 μm. (**d**) Percentage of sPASMCs that are PCNA-positive in *Notch3*$^{-/-}$ and *Notch3*$^{+/+}$ mice (*n* = ten for animals/group, ten lung sections/animal) at timepoints during hypoxia. (**e**) Pulmonary angiograms of *Notch3*$^{-/-}$ and *Notch3*$^{+/+}$ animals after 6 weeks of hypoxia. (**f**) Ratio of the weight of right ventricle (RV), to that of left ventricle plus septum (LV + S), as an index of RV hypertrophy in *Notch3*$^{-/-}$, *Notch3*$^{+/+}$ mice, and *Notch*3$^{+/-}$ mice (for all groups, *n* = 20) after 6 weeks of hypoxia.

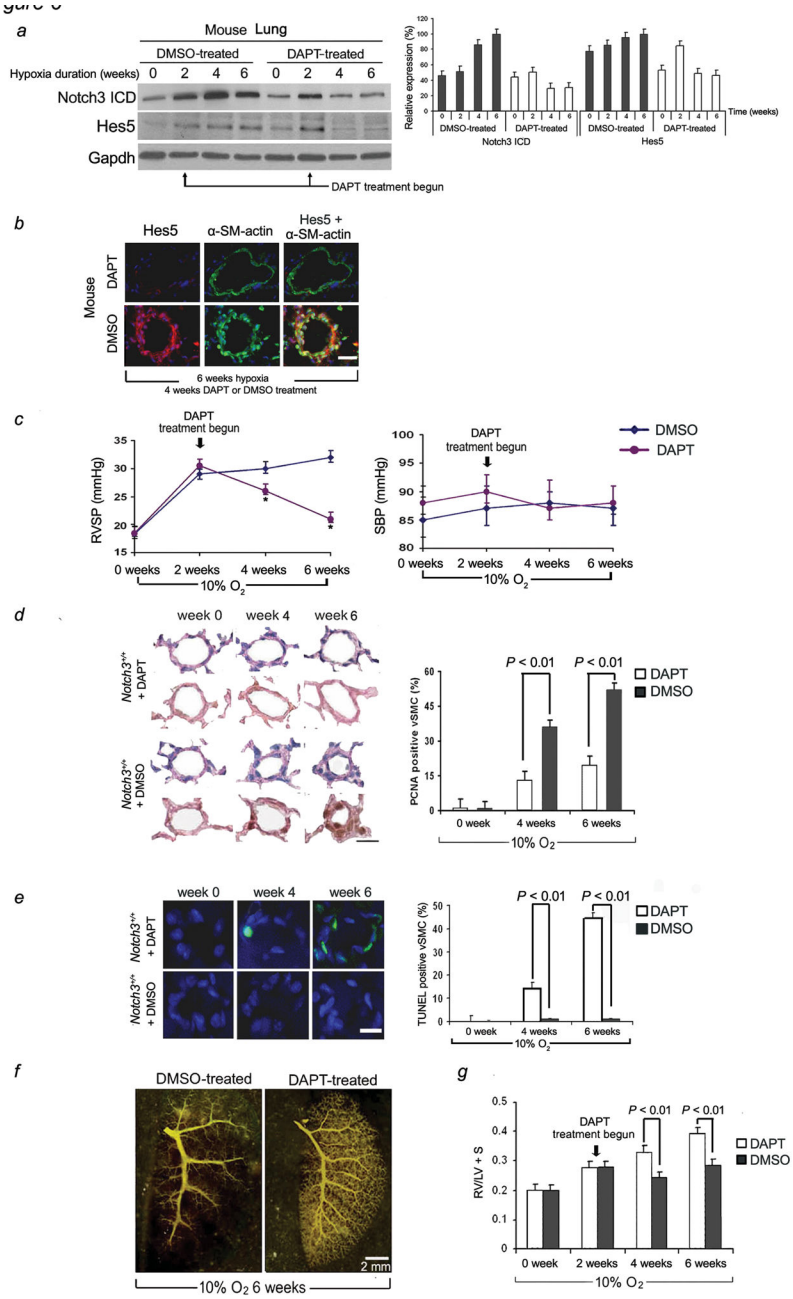

Figure 6.

DAPT treatment reverses the development of hypoxic PH in mice. Animals were exposed to 2 weeks of 10% oxygen, followed by 4 weeks of 10% oxygen and treatment with subcutaneous DAPT or placebo (DMSO). (**a**) Left panel: Western blot analysis of Notch3 ICD and Hes5 in the lungs of mice receiving DAPT as a function of time. Right panel: Relative expression values obtained by densitometry of Notch3 ICD and Hes5 protein normalized to Gapdh (*n* = ten for each timepoint in each group). (**b**) Hes5 (red) and α-SM-actin (green) immunofluorescence staining in small pulmonary arteries from hypoxic mice treated for 4 weeks with DAPT or DMSO. Nuclei are counterstained with DAPI. Scale bar =

25 μm. (**c**) Averaged RVSP (left panel) and SBP (right panel) in mice under hypoxic conditions (ten readings per animal, 20 animals per group at each timepoint). *$P < 0.01$ versus DMSO control. (**d**) Left panel: Hematoxylin and eosin-stained sections (rows one and three) and immunohistochemical analysis of PCNA (rows two and four) of small pulmonary arteries from the lungs of mice after treatment with DAPT or placebo (days 15–42) and 6 weeks of hypoxia. Dark nuclei are PCNA positive. Results are representative sections from five animals per group per timepoint. Scale bar = 25 μm. Right panel: Percentage of sPASMCs that are PCNA-positive in DAPT- and placebo-treated mice in hypoxia. (n = ten animals per timepoint for each group, ten sections/animal). (**e**) Left panel: TUNEL staining (green) with DAPI nuclear staining (blue) in small pulmonary arteries from the same animals lungs as in D. Results are representative sections from five animals per group per timepoint. Scale bar = 25 μm. Right panel: Percentage of sPASMCs that are TUNEL-positive in DAPT- and placebo-treated mice in hypoxia. (n = ten animals per timepoint for each group, ten sections/animal). (**f**) Pulmonary angiograms of DAPT-and placebo-treated animals after 6 weeks of hypoxia. (**g**) Ratio of the weight of right ventricle (RV), to that of left ventricle plus septum (LV + S), as an index of RV hypertrophy in DAPT- (n = 20) versus placebo-treated (n = 20) mice after 6 weeks of hypoxia.